FOLDMATCH: ACCURATE AND HIGH FIDELITY GARMENT FITTING ONTO 3D SCANS

Sk Aziz Ali[⋆†] *Sikang Yan*[⋆] *Wolfgang Dornisch*[‡] *Didier Stricker*[⋆†]

[⋆] TU Kaiserslautern, [†] German Research Center for Artificial Intelligence (DFKI), Germany
[‡] Brandenburgische Technische Universität Cottbus-Senftenberg, Germany

ABSTRACT

In this paper, we propose a new template fitting method that can capture fine details of garments in target 3D scans of dressed human bodies. Matching the high fidelity details of such loose/tight-fit garments is a challenging task as they express intricate folds, creases, wrinkle patterns, and other high fidelity surface details. Our proposed method of non-rigid shape fitting – FoldMatch – uses physics-based particle dynamics to explicitly model the deformation of loose-fit garments and wrinkle vector fields for capturing clothing details. The 3D scan point cloud behaves as a collection of astrophysical particles, which attracts the points in template mesh and defines the template motion model. We use this point-based motion model to derive regularized deformation gradients for the template mesh. We show the parameterization of the wrinkle vector fields helps in the accurate shape fitting. Our method shows better performance than the state-of-the-art methods. We define several deformation and shape matching quality measurement metrics to evaluate FoldMatch on synthetic and real data sets.

Index Terms— Shape Matching, Wrinkle Vector Field, Cloth Simulation, Deformation Gradient, N-body Problem.

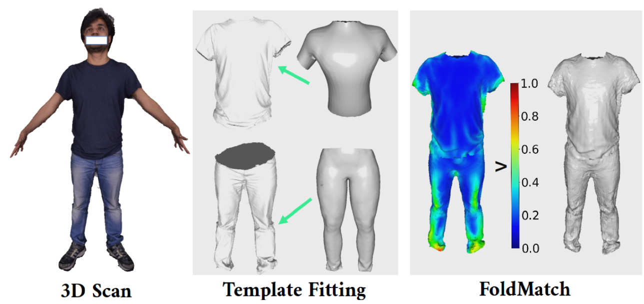

Fig. 1. FoldMatch: A template mesh (*middle*) fitting, as a set of upper and lower garment segments, on a target 3D scan (*left*) of a dressed human body. High fidelity surface details of the registered template are expressed as color-mapped magnitude of wrinkle-vector field v (*right*).

1. INTRODUCTION AND RELATED WORK

Modeling 3D human body with clothes is a primary research domain in 3D computer vision for its exhaustive application in virtual and augmented reality, gaming, and other areas. In this important discipline, statistical models from [1, 2] can reproduce realistic body shapes and poses but without clothes. These models require a large amount of input laser scan data of different subjects with a wide range of motion variation to encode the shape-pose correlation weights. Realistic body shape and pose generative model SMPL [3] extends the boundary with full supervision. Appropriate *Linear Blend skinning* (LBS) for soft body deformation is the underlying objective of these models. The problem of modeling soft body deformation, especially for clothes and garments, is difficult because such deformation has high degrees of freedom. Conformal changes in clothes not only depend on the shift in the underlying pose and shape of the body but also on the physical attributes of the clothing materials. The statistical model of clothing [4] animates well on synthetic bodies, but incomprehensible for realistic body shapes. Recent methods ClothCap [5] and DeepWrinkles [6] advance this field with convolutional neural networks (CNNs) based supervision. These methods [5, 6] require accurate registration of plane garment templates to 4D (3D + time) scan point cloud sequences. In [5], the body-pose, shape-identity and kinematic dependent registration method fits a body model to the scans, whereas the garment priors extract the offset information on the clothing. In [6], variants of non-rigid ICP [7] performs the registration and clothing details are mapped separately via surface normal maps.

In this paper, we introduce a new physics-based conformal registration method, *FoldMatch*, for loose apparels which can match complex folding and pleating patterns of clothes on the target 4D scans as shown in Fig. 1. The proposed method can be more accurate and easy replacement for the non-rigid registration methods applied in [5, 6]. The body of related research works in cloth animation, simulation, deformation analysis, to name a few, is quite vast [8, 9, 10, 11, 12]. Previous deformable shape matching methods like [13, 14] estimate optimal rigid transformation per vertex establishing true point-to-point correspondences. The idea has been further extended in [10] to model deformation as a combination

This work was partially supported by the project VIDETE (01IW18002) of the German Federal Ministry of Education and Research (BMBF).

of linear and quadratic transformations. Similarly, a simulation method for elastoplastic materials with large deformation was addressed in [9]. NRGA [15] is the first physics-based method which applies locally coherent linear transformation per point and the method is robust against noisy target scans. This method works purely on point clouds and consider no vertex connectivity information similar to other widely used methods – CPD [16], non-rigid ICP [7].

Contributions. (1) We identify that NRGA does not have an explicit shape deformation model. It defines a local subspace for every point in the source point cloud, and then a physics based motion model displaces the points independently towards the target point cloud. The displacement field per point is parameterized by rigid rotation $\mathbf{R}$ and translation $\mathbf{t}$. *FoldMatch substantially alters NRGA and defines a deformation model and wrinkle-vector field (WVF) for reproducing drape patterns of a target on a source (a template), which is a mesh.* The target mesh can be noisy scans or reconstructed meshes [17] of dressed human bodies. (2) *Our wrinkle-vector field is parameterized by a stretch coefficient for capturing the drape geometry of the target.* (3) The transformation parameters (rotation and translation) for every template point are *optimally estimated directly from the regularized deformation gradient, which contains additional cues of the desirable drapes*. (4) We propose several *error metrics to quantitatively evaluate the matching accuracy of FoldMatch against SoA registration methods and analyze the WVF for different spreads of local subspace*.

2. NON-RIGID GRAVITATIOINAL APPROACH

Given a template $\mathbf{Y}$ and a reference $\mathbf{X}$, The gravitational approach for non-rigid point set registration – NRGA [15] defines the Gravitational Potential Energy (GPE) of the system:

$$\mathbf{E}(\mathbf{R},\mathbf{t}) = -\sum_{k=1}^{M}\sum_{j\in\Gamma_k^{\mathbf{X}}} \frac{\omega_k}{(\|\mathbf{R}_k\mathbf{Y}_k + \mathbf{t}_k - \mathbf{X}_j\| + \epsilon)}, \quad (1)$$

which is the weighted (ω_k) sum of the inverse of the euclidean distances ($\|.\|$ denotes ℓ_2 norm) between the vertices $\mathbf{Y} = [\mathbf{Y}_1, \mathbf{Y}_2, \ldots, \mathbf{Y}_M]$ and their neighboring vertices from $\mathbf{X} = [\mathbf{X}_1, \mathbf{X}_2, \ldots, \mathbf{X}_N]$. From the definition of GPE, the weight ω_k stands as the product of the *gravitational constant* G and the masses $(m(\mathbf{Y}_k), m(\mathbf{X}_j))$ of interacting vertex pair $(\mathbf{Y}_k, \mathbf{X}_j)$. The above energy in eq. (1) is minimized to estimate the optimum transformation parameters, *i.e.,* M rotations $\mathbf{R} = [\mathbf{R}_1, \ldots, \mathbf{R}_M]$ and translations $\mathbf{t} = [\mathbf{t}_1, \ldots, \mathbf{t}_M]$ for the template vertices. By applying the rigid transformations, $\mathbf{Y}$ deforms to match the underlying shape of $\mathbf{X}$.

Optimization Technique. NRGA uses distributed N-body system as an inverse-problem toolbox to minimize the energy in Eq. (1). The method applies some constraints as – (A) there are no interactions among the particles from same class, *i.e.,* $\mathbf{X}$ or $\mathbf{Y}$, (B) only $\mathbf{X}$ induces gravitational forces to attract $\mathbf{Y}$, and (C) interactions are collisionless. First, K-d trees are built independently on source $\mathbf{Y}$ and target $\mathbf{X}$ which help obtaining the nearest neighbors of every source vertex $\mathbf{Y}_k$. Every $\mathbf{Y}_k$ fetches a number of nearest neighbors from $\mathbf{Y}$ and target $\mathbf{X}$ as a proportion ρ (typically $0.02 - 0.2\%$) of their total points. These neighbors form local regions $\Gamma_k^{\mathbf{Y}}$, $\Gamma_k^{\mathbf{X}}$, respectively. This generates a number of corresponding region-pairs $((\Gamma_1^{\mathbf{Y}}, \Gamma_1^{\mathbf{X}}), \ldots, (\Gamma_M^{\mathbf{Y}}, \Gamma_M^{\mathbf{X}}))$ equal to the number of points in $\mathbf{Y}$. Next, the method iterates over all region-pairs and computes the cumulative sum of *relativistic gravitational force* (RGF) [18, 19] $\mathbf{F}_k$ on every $\mathbf{Y}_k \in \Gamma_k^{\mathbf{Y}}$ from all $\mathbf{X}_j \in \Gamma_k^{\mathbf{X}}$, velocity $\mathbf{v}_k^{t+\Delta t}$, and displacement $\mathbf{d}_k^{t+\Delta t}$ as:

$$\mathbf{F}_k = -\sum_{j\in\Gamma_k^{\mathbf{X}}} \frac{\omega_k(\mathbf{Y}_k\alpha_{kj} - \mathbf{X}_j)}{\left(\|\mathbf{Y}_k - \mathbf{X}_j\|^2 + \epsilon^2\right)^{3/2}\alpha_{kj}^{3/2}} - \eta\mathbf{v}_k^t, \quad (2)$$

$$\mathbf{v}_k^{t+\Delta t} = \mathbf{v}_k^t + \frac{\mathbf{F}_k}{m(\mathbf{Y}_k)}\Delta t \text{ and } \mathbf{d}_k^{t+\Delta t} = \mathbf{v}_k^{t+\Delta t}\Delta t. \quad (3)$$

$\mathbf{F}_k$ is parameterized by the Gaussian curvature [20] κ_j of $\mathbf{X}_j$ as the term $\alpha_{kj} = 1 - \frac{1}{2}\kappa_j\|\mathbf{Y}_k - \mathbf{X}_j\|^2$. The phase-space of $\mathbf{Y}$ is defined by M position ($\mathbf{Y}_k$) and velocity ($\mathbf{v}_k$) vectors at time-step t. A fraction, η, of velocity is dissipated to stop the endless oscillation due to second-order ordinary differential equations (ODEs) of motion in Eq. 2 and 3. The rotations $\mathbf{R}$ and translations $\mathbf{t}$ are estimated from the previous and updated positions of vertices in the regions. The method terminates when number of iterations exceeds a threshold ξ.

3. THE PROPOSED GARMENT FITTING METHOD

The template cloth in our proposed method is a mesh containing a set of vertices and triangular faces $\mathcal{T}$. Next, Using the positional dynamics of template points (particles with masses) defined in Eq. 2, we derive deformation gradient and introduce wrinkle-vector field.

Smooth Deformation Gradient. The vertices under the region $\Gamma_k^{\mathbf{X}}$ are a set of $\lfloor\rho N\rfloor$ nearest neighbors from $\mathbf{X}$, whereas vertices under $\Gamma_k^{\mathbf{Y}}$ are a set of distinct vertices connected inside 2 or 3-path distance from $\mathbf{Y}_k$. Fig. 2 describes how the current state $(\mathbf{Y}_k^t, \mathbf{v}_k^t)$ and next state $(\mathbf{Y}_k^{t+\Delta t}, \mathbf{v}_k^{t+\Delta t})$ of the vertices enclosed by any $\Gamma_k^{\mathbf{Y}}$ reflect subspace deformation. The continuum deformation gradient:

$$\mathbf{H}_k = (\sum_{j\in\Gamma_k^{\mathbf{Y}}} \beta_j(\mathbf{Y}_j^{t+\Delta t} - \mathbf{Y}_j^{\bar{t}+\Delta t}) \otimes \delta\mathbf{Y}_j^t)(\sum_{j\in\Gamma_k^{\mathbf{Y}}} \beta_j\delta\mathbf{Y}_j^t \otimes \delta\mathbf{Y}_j^t)^{-1} \quad (4)$$

of $\mathbf{Y}_k$ is formulated using the principle of molecular dynamics [21] with $\beta_j = \frac{1}{|j|}$. The determinant of $\mathbf{H}_k$ is non-singular when the term $(\sum_{j\in\Gamma_k^{\mathbf{Y}}} \beta_j\delta\mathbf{Y}_j^t \otimes \delta\mathbf{Y}_j^t)^{-1}$ exists, *i.e,* when a non-linear or non-flat stretch occurs inside $\Gamma_k^{\mathbf{Y}}$. First we obtain $\mathbf{H}_k$ for all $\mathbf{Y}_k \in \mathbf{Y}$ using Eq. (4). Thereafter, we regularize $\mathbf{H}_k$ using tensor interpolation [22] scheme:

$$\mathbf{H}_k = \mathbf{H}_k^{\frac{1}{2}} \exp\left(\sum_{j\in\Gamma_k^{\mathbf{Y}}} \beta_j \log(\mathbf{H}_k^{\frac{-1}{2}}\mathbf{H}_j\mathbf{H}_k^{\frac{-1}{2}})\right)\mathbf{H}_k^{\frac{1}{2}}. \quad (5)$$

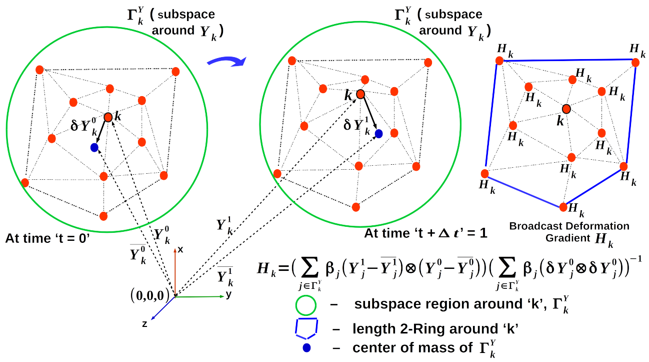

Fig. 2. Geometric deformation is captured for every vertex $\mathbf{Y}_k$ (in red) of the template mesh $\mathbf{Y}$. Deformation gradient $\mathbf{H}_k$ of $\mathbf{Y}_k$ quantifies the gradient of motion locally around $\mathbf{Y}_k$. The relative change in the position of $\mathbf{Y}_k$ with respect to the adjacent points in its subspace (*enclosed by green circles*) at time-steps t and $t+\Delta t$ of simulation are used to compute $\mathbf{H}_k$. These $\mathbf{H}_k$ are broadcast to those nearest neighbor points (*enclosed by the blue polygon*) to be interpolated for final update. $\mathbf{Y}_k$ selects n-ring neighborhood vertices, reachable from $\mathbf{Y}_k$ with the shortest-path-length $\leq n$, to define $\Gamma_k^{\mathbf{Y}}$.

A more convenient deformation measure is the *Right Cauchy-Green Deformation* (RCGD) tensor $\mathbf{C}$ as $\mathbf{C}_k = \mathbf{H}_k^T\mathbf{H}_k$. The RCGD tensor is related to the stretch tensor $\mathbf{U}_k$ as:

$$\mathbf{C}_k = \mathbf{H}_k^T\mathbf{H}_k = (\mathbf{R}_k\mathbf{U}_k)^T(\mathbf{R_k}\mathbf{U_k}) = \mathbf{U}_k^T\mathbf{R}_k^T\mathbf{R}_k\mathbf{U}_k = \mathbf{U}_k^2. \tag{6}$$

Wrinkle-Vector Field. Thanks to the smoothly interpolated $\mathbf{H}_k$ in Eq. (5), polar decomposition of $\mathbf{H}_k$ results to a smooth Rigid Rotation Tensor $\mathbf{R}_k$ and a smooth Stretch Tensor $\mathbf{U}_k$. The eigen value decomposition of $\mathbf{U}_k = \sum_{i=1}^{3}\lambda_i e_i e_i^T$ gives principal stretch λ_1 (as $\mathbf{C}_k = \sum_{i=1}^{3}\lambda_i^2 e_i e_i^T$) and its direction e_1. Some methods [23, 8] influence the stretch-tensor in cloth-simulation by clamping or trimming its principal eigen value λ_1. We add a stretch coefficients ψ along the principal direction e_1 and reduce proportionately from other two directions e_2, e_3 to increase the proportion drape cues. The modified eigen become: $\hat{\lambda}_1 = \frac{1}{s}(\lambda_1+\psi)$, $\hat{\lambda}_2 = \frac{1}{s}(\lambda_2-\frac{\psi}{2})$, and $\hat{\lambda}_3 = \frac{1}{s}(\lambda_3-\frac{\psi}{2})$, where $s = (\frac{(\lambda_1+\psi)^2+(\lambda_2-\frac{\psi}{2})^2+(\lambda_3-\frac{\psi}{2})^2}{3})^{\frac{1}{2}}$. Hence our modified stretch tensor is $\hat{\mathbf{U}}_k = \sum_{i=1}^{3}\hat{\lambda}_i e_i e_i^T$. Next, We define the wrinkle-vector field v as:

$$v = \left(\frac{\lambda_1+\psi}{s}\right)e_1 = \hat{\lambda}_1 e_1. \tag{7}$$

Resolving Transformation Per-Point. The final step of FoldMatch is to resolve the rotation by optimizing the following constrained co-rotational problem:

$$\mathbf{R}_k^* = \arg\min_{\hat{\mathbf{R}}_k}\|\mathbf{H}_k - \hat{\mathbf{R}}_k\hat{\mathbf{U}}_k\|_F^2, \quad \text{s.t} \quad \hat{\mathbf{R}}_k^T\hat{\mathbf{R}}_k = \mathbf{I}, \tag{8}$$

where $\|.\|_F$ denotes Frobenius norm. Once the optimal rotation $\mathbf{R}_k^*$ for $\mathbf{Y}_k$ is obtained, the optimal translation is estimated as $\mathbf{t}_k^* = \bar{\mathbf{Y}}_k^{t+\Delta t} - \mathbf{R}_k^*\bar{\mathbf{Y}}_k^t$. M rotations and translations deform our template at every time-step. The method terminates after maximum number of allowed iterations ξ. In the end, the template $\mathbf{Y}$ is deformed to its final state $\hat{\mathbf{Y}}$.

4. EXPERIMENTS AND EVALUATION

In all the experiments, the parameters required for the N-body simulation part are set as: $G = 1.67$, $\epsilon = 0.1$, $\eta = 0.1$, $\Delta t = 0.006$, $m(\mathbf{Y}_k) = 1.0$, $m(\mathbf{X}_j) = 1.0$, $\xi = 100$, and for the cloth deformation, the wrinkle stretch parameter $\psi = 0.05$. We quantify the matching quality of our method tested on some synthetic [24] and real [25, 26] data sets, and compare them against three benchmark methods of point-set registration – CPD [16], NRICP [7] and NRGA [15].

Evaluation Metric. Without known ground truth correspondences between template and target garments, quantifying geometric deformation and matching accuracy is difficult. We use a combined metric f_λ as an average on – (1) the ratio of Hausdorff distances $f_{\mathbf{H}}$ before and after registration as $f_{\mathbf{H}} = \mathcal{D}_{\mathbf{H}}(\mathbf{X},\widehat{\mathbf{Y}})/\mathcal{D}_{\mathbf{H}}(\mathbf{X},\mathbf{Y})$, (2) the fraction $f_{\mathbf{S}}$ of triangular faces $\mathcal{T}$ in $\mathbf{Y}$ collapsed into some infinitesimal area when the area shrinkage is smaller than a threshold $\tau = 0.02$, $f_{\mathbf{S}} = \frac{1}{|\mathcal{T}|}\sum_{(i,j,k)\in\mathcal{T}}\mathbb{1}(\widehat{\Delta}_{ijk}/\Delta_{ijk} < \tau)$, (3) the fraction of faces with large rate of expansion $f_{\mathbf{E}}$ is the opposite measurement of shrinkage $f_{\mathbf{S}} = \frac{1}{|\mathcal{T}|}\sum_{(i,j,k)\in\mathcal{T}}\mathbb{1}(\widehat{\Delta}_{ijk}/\Delta_{ijk} > \tau)$, $\tau = 2.0$, (4) the fraction of flipped triangles $f_{\mathbf{F}}$ which measures if the angle greater than 90° between them before and after, resulting in a scalar product of their normal vectors below zero: $f_{\mathbf{F}} = \frac{1}{|\mathcal{T}|}\sum_{i\in\mathcal{T}}\mathbb{1}(n_i^T\widehat{n}_i < 0)$. and finally, (5) the RMSE error $f_{\mathbf{R}}$ on the distances from the ground truth correspondences, if available, – as $f_\lambda = \frac{(f_{\mathbf{H}}+f_{\mathbf{S}}+f_{\mathbf{E}}+f_{\mathbf{F}}+f_{\mathbf{R}})}{5}$.

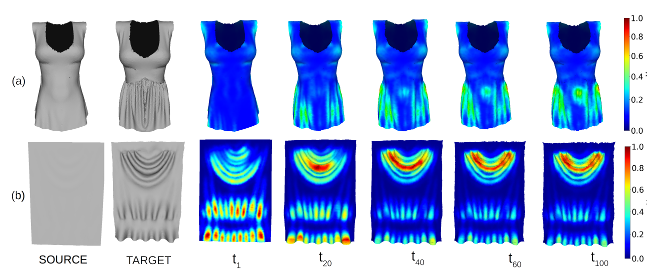

Fig. 3. Experimental results with simulation steps of our method on two different types garment samples from [24].

On Synthetic Data. FoldSketch [24] requires some input configurations for stitching disjoint segments of the garment to generate desired folding, pleating, and hemline patterns intuitively. We collect those disjoint segments and merge them to get *twelve* input-output sets for our experiments – *chipao, conjoined, complex dress, flag*, to name a few. Fig. 3 shows the qualitative results of our method. Template and target contain $\approx 13K$ and $\approx 14K$ points for the *flag* and *complex dress*, respectively. FoldMatch converges in $\sim 30-40$ iterations (runtime: 3.5 mins) and the neighborhood boundaries

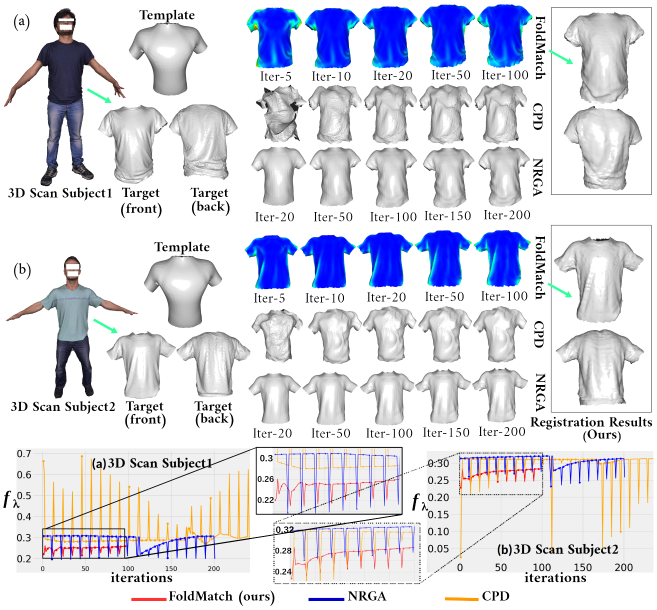

Fig. 4. A single template of 'shirt', without any surface details, is fitted on two scans with different drape patterns. FoldMatch converges faster and results in capturing more accurate surface details than CPD and NRGA.

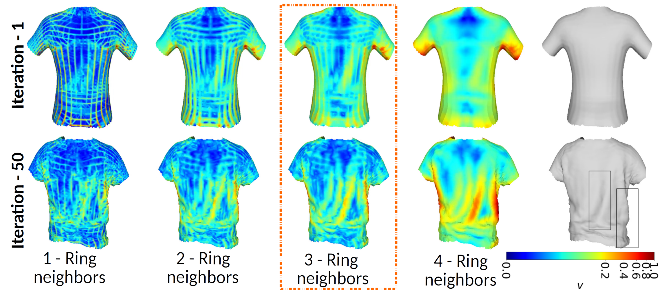

Fig. 5. Deciphering sharpness of wrinkles from the deformation gradient for different spreads (n-ring) of subspace $\Gamma_k^{\mathbf{Y}}$.

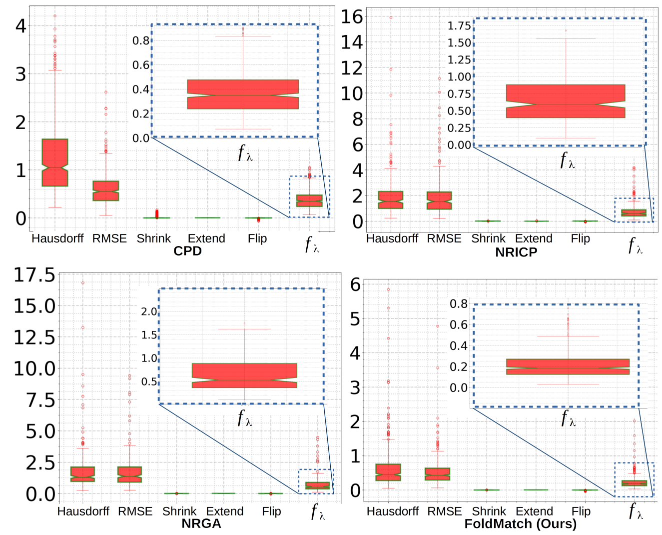

Fig. 6. Quantitative evaluation of FoldMatch (ours), CPD, NRICP and NRGA methods on 300 samples from the training data set [26]. Ours has the lowest of max-error values on all evaluation metrics $f_{\mathbf{H}}$, $f_{\mathbf{S}}$, $f_{\mathbf{E}}$, $f_{\mathbf{F}}$, $f_{\mathbf{R}}$, and f_λ (as avg. of all).

$\Gamma_k^{\mathbf{Y}}$ and $\Gamma_k^{\mathbf{X}}$ for $\mathbf{Y}_k$ are kept to 2-ring (covers $\approx$0.2% of total points $13K$ in the template) and 0.2% points from the target.

On Real Data. **(1)** The first set of experiments quantitatively evaluate the deformable registration accuracy of FoldMatch when performed on some dressed-human body scans from [25]. Fig. 4 summarizes the registration quality of our FoldMatch, where the 'shirt'of both scan subjects captures all wrinkle and drape patterns close to the target scans. Our method converges quickly after $\sim 20 - 30$ iterations, whereas CPD and NRGA take more than $\sim 150 - 200$ iterations to reach a state where either the template mesh is deformed incorrectly or capture coarser details of the wrinkle patterns. The plots in Fig. 4 show that our method gradually optimizes achieving the deformation state with the lowest values of f_λ for both subjects. For more analysis, Fig. 5 picks the 'subject1' from Fig. 4 and shows how the wrinkle vector fields, v, are either locally sharpen or diffused when different sizes of ring neighbors ($\Gamma_k^{\mathbf{Y}}$) – 1-ring, 2-ring, 3-ring, and 4-ring – deciphering more information from respective $\mathbf{H}_k$.

(2) Another set of experiments uses a large training data [26] of a flat-piece of deformable clothes. [26] contains five different garments – cloth, T-shirt, hoody, sweater, and paper, but only *cloth* contains ground truth meshes for $\sim$15799 samples. FoldMatch is tested on a subset of 300 randomly selected samples as target meshes except for the first sample as template mesh. Fig. 5 reflects the distribution of the quantitative error metric f_λ, including its different components ($f_{\mathbf{H}}$, $f_{\mathbf{S}}$, $f_{\mathbf{E}}$, $f_{\mathbf{F}}$, $f_{\mathbf{R}}$), for *FoldMatch*, CPD, NRICP and NRGA. The third quantiles of maximum error are 0.8, 1.55, and 1.6 for CPD, NRICP, and NRGA, respectively. These errors are $\sim$1.5 times and $\sim$3 times higher than our FoldMatch. The outliers' ranges are worse for NRICP and NRGA.

5. CONCLUSIONS AND FUTURE WORK

Our method is a new mesh fitting method for capturing high fidelity details of the target scans. It allows analyzing patterns of wrinkles or creases from the locally smooth deformation gradients and wrinkle vector fields, which can further help in relating human body motion primitives with garment deformations statistics. Our method outperforms NRGA, CPD, and NRICP in capturing intricate details of clothes. FoldMatch can be a natural replacement for widely used NRICP or other alignment methods in any cloth capturing or reconstruction pipeline. In the future, we plan to employ acceleration techniques for fast force computation on a GPU, and then to generate pseudo ground truth meshes of input 4D scan sequences.

6. REFERENCES

[1] N. Hasler, C. Stoll, M. Sunkel, B. Rosenhahn, and H.P. Seidel, "A statistical model of human pose and body shape," *Computer Graphics Forum*, vol. 28, no. 2, pp. 337–346, 2009.

[2] D. Anguelov, P. Srinivasan, D. Koller, S. Thrun, J. Rodgers, and J. Davis, "Scape: shape completion and animation of people," *ACM TOG*, vol. 24, pp. 408–416, 2005.

[3] M. Loper, N. Mahmood, J. Romero, G. Pons-Moll, and M. J. Black,, "SMPL: A skinned multi-person linear model," *ACM TOG (Proc. SIGGRAPH Asia)*, vol. 34, no. 6, pp. 248:1–248:16, 2015.

[4] P. Guan, L. Reiss, D. Hirshberg, A. Weiss, and M. Black, "DRAPE: DRessing Any PErson," *ACM Trans. on Graphics (Proc. SIGGRAPH)*, vol. 31, no. 4, pp. 35:1–35:10, July 2012.

[5] G. Pons-Moll, S. Pujades, S. Hu, and M. Black, "Clothcap: Seamless 4d clothing capture and retargeting," *ACM TOG, (Proc. SIGGRAPH)*, vol. 36, no. 4, 2017.

[6] Z. Lahner, D. Cremers, and T. M. Tung, "Deepwrinkles: Accurate and realistic clothing modeling," in *ECCV*, 2018.

[7] B. Amberg, S. Romdhani, and T. Vetter, "Optimal step nonrigid icp algorithms for surface registration," in *IEEE Conference on Computer Vision and Pattern Recognition (CVPR)*, 2007.

[8] D. Rohmer, T. Popa, M.-P. Cani, S. Hahmann, and A. Sheffer, "Animation wrinkling: Augmenting coarse cloth simulations with realistic-looking wrinkles," *ACM TOG*, vol. 29, no. 6, 2010.

[9] G. Irving, J. Teran, and R. Fedkiw, "Invertible finite elements for robust simulation of large deformation," in *ACM SIGGRAPH*, 2004.

[10] M. Müller, B. Heidelberger, M. Teschner, and M. Gross, "Meshless deformations based on shape matching," *ACM transactions on graphics (TOG)*, 2005.

[11] J. Yang, J. Franco,, F. Hétroy-Wheeler,, and S. Wuhrer, "Analyzing clothing layer deformation statistics of 3d human motions," in *ECCV*, 2018.

[12] C. Papazov, and D. Burschka, "Deformable 3d shape registration based on local similarity transforms," in *Computer Graphics Forum*. Wiley Online Library, 2011, vol. 30, pp. 1493–1502.

[13] P. J. Besl and N. D. McKay, "A method for registration of 3d shapes," *IEEE Transactions on Pattern Analysis and Machine Intelligence*, 1992.

[14] M. Kazhdan, T. Funkhouser, and S. Rusinkiewicz, "Shape matching and anisotropy," in *ACM TOG*, 2004.

[15] Sk. A. Ali, V. Golyanik, and D. Stricker, "Nrga: Gravitational approach for non-rigid point set registration," *International Conference on 3D Vision (3DV)*, pp. 756–765, 2018.

[16] A. Myronenko and X. Song, "Point set registration: Coherent point drift," *IEEE Transactions on Pattern Analysis and Machine Intelligence*, 2010.

[17] J. Gall, C. Stoll, E. De Aguiar, C. Theobalt, B. Rosenhahn, H.-P. Seidel, "Motion capture using joint skeleton tracking and surface estimation," in *2009 IEEE Conference on Computer Vision and Pattern Recognition (CVPR)*, 2009.

[18] F. Diacu, "The classical n-body problem in the context of curved space," *Canadian Journal of Mathematics*, vol. 69, pp. 790–806, 2017.

[19] C. M. Will, *Gravity: Newtonian, Post-Newtonian, and General Relativistic*, pp. 9 – 72, Springer International Publishing, 2016.

[20] P. Yang, X. Qian, "Direct computing of surface curvatures for point-set surfaces.," in *Eurographics Symposium on Point-Based Graphics (SPBG)*, 2007.

[21] L. Zhang, J. Jasa, G. Gazonas, A. Jérusalem, and M. Negahban, "Extracting continuum-like deformation and stress from molecular dynamics simulations," *Computer Methods in Applied Mechanics and Engineering*, vol. 283, pp. 1010 – 1031, 2015.

[22] X. Pennec, P. Fillard, and N.Ayache,, "A riemannian framework for tensor computing," *International Journal of computer vision*, vol. 66, no. 1, pp. 41–66, 2006.

[23] R. Narain, A. Samii, and J. F. O'Brien, "Adaptive anisotropic remeshing for cloth simulation," *ACM TOG*, vol. 31, no. 6, pp. 147:1–10, 2012.

[24] M. Li, A. Sheffer, E. Grinspun, and N. Vining, "Foldsketch: Enriching garments with physically reproducible folds," *ACM TOG*, vol. 37, no. 4, 2018.

[25] V. Golyanik, G. Reis, B. Taetz, and D. Strieker, "A framework for an accurate point cloud based registration of full 3d human body scans," in *IAPR MVA*, 2017.

[26] J. Bednarik, P. Fua, and M. Salzmann, "Learning to reconstruct texture-less deformable surfaces from a single view," in *2018 International Conference on 3D Vision (3DV)*, 2018.